γ decay of excited states in ^{198}Rn identified using correlated radioactive decay

R. B. E. Taylor, S. J. Freeman, J. L. Durell, M. J. Leddy, S. D. Robinson, and B. J. Varley
Schuster Laboratory, University of Manchester, Manchester M13 9PL, United Kingdom

J. F. C. Cocks, K. Helariutta, P. Jones, R. Julin, S. Juutinen, H. Kankaanpää, A. Kanto, H. Kettunen, P. Kuusiniemi, M. Leino, M. Muikku, P. Rahkila, and A. Savelius
Department of Physics, University of Jyväskylä, Jyväskylä, Finland

P. T. Greenlees
Oliver Lodge Laboratory, University of Liverpool, Liverpool, United Kingdom
(Received 25 August 1998)

The low-lying level structure of the neutron-deficient isotope ^{198}Rn has been studied for the first time, using the ^{166}Er(^{36}Ar,4n) reaction at a beam energy of 175 MeV. Evaporation residues were selected using an in-flight gas-filled separator, RITU, and implanted at the focal plane into a 16-element position-sensitive, passivated ion-implanted planar silicon detector. Prompt γ rays in ^{198}Rn were observed at the target position using the JUROSPHERE array of 24 Compton-suppressed germanium detectors, and were identified by the subsequent radioactive decay of associated recoiling ions in the silicon detector. Isotopic assignments of the nuclei produced were made on the basis of the energy and half-life of their α decay. The estimated production cross section for ^{198}Rn in this reaction was 180 nb. The excitation energy of the 2_1^+ state indicates inconsistency with theoretical predictions of large stable ground-state deformation in this isotope. The systematics of other low-lying excited states suggests the presence of deformed intruder states falling in energy with increasing neutron deficiency. [S0556-2813(99)07802-4]

PACS number(s): 27.80.+w, 23.20.Lv, 23.60.+e

I. INTRODUCTION

The polarization of the doubly magic ^{208}Pb core by valence nucleon particles has been known for many years to be responsible for the permanent deformation exhibited in the ground states of nuclei with $N>126$ and $Z>82$. A new region of deformed nuclei is expected when polarization by proton particles and neutron holes is sufficient to perturb the spherical core. The onset of deformation in this region, where $N<126$ and $Z>82$, has been predicted to occur far from stability by many long-standing calculations [1–4], although no direct experimental evidence exists with which to substantiate these results.

Production of neutron-deficient nuclei via fusion-evaporation reactions becomes increasingly difficult far from stability because of the overwhelming dominance of fission channels over particle emission at every stage of the cooling of the compound nucleus. As a result there is not much experimental information on many of these nuclei other than the ground-state radioactive decay half-life and Q value, which are difficult to interpret in terms of nuclear deformation. Spectroscopy of excited states, where a low 2_1^+ excitation energy or development of rotational band structures might be suggestive of collective effects, is difficult due to the low production cross sections, which fall into the sub-μb regime where the deformation is predicted to be largest. Additional experimental problems arise due to contamination by fission products and Coulomb excitation. This paper presents experimental measurements concerning γ-ray transitions between excited states in ^{198}Rn, an isotope with a large predicted deformation parameter, $|\epsilon_2|\sim 0.2$, but produced in suitable reactions with cross sections of the order of only 100 nb.

II. EXPERIMENTAL DETAILS

The production cross section of ^{198}Rn in the current reaction was estimated from the current work to be only 180 nb, while the total fusion cross section is of the order of 100 mb. A very sensitive technique is thus required to isolate in-beam γ rays deexciting states in evaporation residues surviving fission, from radiation associated with the myriad fission fragments produced. Strong Coulomb excitation of target nuclei of up to a barn in cross section exacerbates the problem. In addition to the rejection of these strong background channels, any γ rays emitted by surviving evaporation residues must be positively identified with ^{198}Rn since there is no published information concerning excited states in this isotope.

In the present study an in-flight gas-filled separator is used to select evaporation residues recoiling out of the target from an unreacted beam. Identification of ^{198}Rn residues was performed on the basis of the radioactive α decay of the residues in a silicon detector at the focal plane of the separator. The decay properties of ^{198}Rn have been established previously [5,6] and the decay proceeds by the emission of an α particle of energy 7.196 MeV with a half-life of 64(2) ms. Prompt γ rays at the target position were identified as transitions between excited states in ^{198}Rn by a correlation technique: γ rays are observed in coincidence with recoiling ions, which, after transportation through the separator and

implantation into a suitable detector, decay by emitting radioactivity with characteristics corresponding to the isotope of interest.

For this investigation ^{198}Rn was produced in the ^{166}Er(^{36}Ar,4n) reaction. A self-supporting metallic target, of thickness 500 μg cm^{-2} and enriched to $>$96% in ^{166}Er, was bombarded with a beam of $^{36}Ar^{7+}$ ions at an energy of 175 MeV, delivered by the K130 cyclotron at the Accelerator Laboratory of the University of Jyväskylä. In order to produce sufficient information for position matching and energy correction, discussed in detail below, the same target was bombarded with an $^{40}Ar^{7+}$ beam at an energy of 192 MeV. The production cross sections with this second reaction lead to less neutron-deficient isotopes and quickly generate enough data for the required corrections.

Prompt electromagnetic radiation emitted at the reaction site was detected in the JUROSPHERE array. The array consisted of 24 Compton-suppressed hyperpure germanium detectors arranged in four rings around the beam direction, surrounding the target position. The array was composed of Ge crystals of two different sizes: fourteen 70% efficient detectors of the EUROGAM phase I type [7], nine at 134° and five at 158° to the forward beam direction, and ten 25% detectors of the TESSA type [8], five each at 79° and 101°. Efficiencies are quoted relative to the NaI standard. The absolute photopeak efficiency of the coaxial detectors in the array was measured to be 1.7% at 1332 keV.

Recoiling evaporation residues were separated from unreacted primary beam particles, fission fragments, and target-like reaction products using the high-efficiency gas-filled recoil separator RITU [9]. This device achieves high transmission by filling the field region of a magnetic dipole with gas at low pressure. Charge-exchanging collisions between recoiling ions and gas atoms lead to ion trajectories centered on the average ionic charge state in the gas, independent of the original charge state when leaving the target. Simple empirical descriptions of the average charge state indicate that the magnetic rigidity of the ion in the gas-filled region is effectively independent of charge state and recoil velocity [10], which leads to a charge and velocity focusing giving high transmission. RITU was filled with helium gas at a pressure of 1 mbar. The helium was isolated from the accelerator vacuum by a thin carbon foil of thickness 50 μg cm^{-2} upstream of the target position.

At the focal plane of RITU, separated ions were stopped in a position-sensitive passivated ion-implanted planar silicon detector. The detector was 35 mm high and 80 mm wide with a thickness of 300 μm. The width was subdivided into 16 strips of width 5 mm. Signals from the top and bottom of each strip, in addition to a summed signal, were recorded. The summed signal was used as an energy measurement, while vertical position along the strip was derived on the basis of the resistive division in off-line analysis of the data. The position measurement was used in the analysis to spatially correlate the arrival of a recoiling ion with its subsequent α decay. Energy and position signals were recorded for events corresponding to the implantation of recoiling ions into the silicon detector and for their subsequent decays. Two sets of amplifiers were used, one with low gain (referred to below as ''recoil'' amplifiers) suitable for the energies associated with recoiling ions (10–40 MeV) and high gain (''decay'' amplifiers) suitable for α-particle energies (5–7 MeV). The α-decay events and implantation events were distinguished on the basis of the recorded energy signal.

Several logical event triggers were generated. A silicon detector trigger was used corresponding to an event in the silicon detector. A recoil-γ trigger was defined by the coincident detection of one or more prompt γ rays in the germanium array around the target and a signal in one of the strips of the silicon detector. In addition, the coincident firing of three or more detectors in the germanium array was used to trigger the data acquisition system. This latter trigger was used for diagnostic purposes to allow on-line monitoring of the detectors in the array.

Along with the other experimental parameters of the event, the time at which the event occurred was recorded. This was generated by a scaler which ran continuously throughout the duration of the experiment. This scaler was interrogated every time a trigger of any sort was received by the data acquisition system. Events were thus labeled with the time at which they occurred, relative to the beginning of the experiment, at a precision of 1 μs. This time label allows the data to be played back in sequential order during off-line sorting to build up temporal correlations between the events occurring at each position in the silicon detector.

Data were collected for approximately 154 h at an average beam current of 10 pnA, giving an average raw rate of 30–40 Hz in the silicon detector. The beam current used was limited by the rate in the germanium detectors, which was typically a 3–4 kHz Compton-suppressed rate per 70% detector and 2–3 kHz per 25% detector.

III. DATA REDUCTION AND ANALYSIS

In order to begin the analysis, the various detector elements require gain matching and conditions to be applied to the data set require determination. The germanium detectors were calibrated by collecting singles γ-ray energy spectra from ^{152}Eu and ^{133}Ba sources, giving good coverage of the energy range of interest. These were used to obtain gain-matching coefficients and to perform a relative efficiency calibration for the 24 coaxial germanium detectors in singles mode. A Doppler-shift energy correction was applied to the in-beam γ-ray data using a calculated value of recoil velocity, $\beta = v/c = 0.0183$, assuming ions recoil at 0°. A calculated recoil velocity was used since the number of counts in any one γ-ray transition in any one angular ring of detectors was too small to deduce an empirical Doppler correction to the data. The JUROSPHERE array has most of its efficiency towards the backward angles and as such the use of a calculated recoil velocity introduces a systematic error into the measurements of γ-ray energies. This is estimated to be less than $\sim$0.3 keV at 500 keV.

Transformations were made of the α-particle energy signals in order to correct for a small linear dependence of the observed energy with vertical position. This was performed using strong α groups arising from the decay of ^{201m}Rn and ^{198}Po produced in the ^{40}Ar-induced reaction. An energy resolution of 26–30 keV was typically obtained in an individual strip after correction. The strips were gain matched

and an internal energy calibration was performed using known α-particle energies in order to confirm the identification of lines in the energy spectrum.

Since independent banks of amplifiers were used, the position signal derived from the ''recoil'' amplifiers needs matching to that derived from the ''decay'' amplifiers. In order to match the two position measurements, the $^{201m/201}$Rn activities, strongly produced in the ^{40}Ar reaction, were used. The α decays corresponding to previous implantations were searched for and a two-dimensional plot of decay position versus recoil position was incremented. The true recoil-α correlations produce a line in such a plot, on top of a background due to false, chance correlations. A linear transformation was applied in order to put the true correlations onto the diagonal in the two-dimensional plot and thus match the gains of the two position measurements. Position resolution was typically found to be $\sim$400 μm full width at half maximum (FWHM).

The analysis is based on the observation of time- and position-correlated implantation and α decays in the silicon detector. Since some of the implantation events will involve the detection of prompt γ rays at the target position, the identification of the α-decay characteristics of a particular isotope allows a specific selection and identification for prompt γ rays emitted by that isotope. Such analysis involves an off-line search through the collected data to find the α decay corresponding to implantation at a particular position, seen in the silicon detector. The two events are deemed to have occurred at the ''same'' position in the detector if their two position measurements are within ± 1 FWHM position resolution. The time interval between the implantation and decay is used to measure the half-lives of the isotopes produced.

In order to establish good correlated events, the mean life of an implanted ion should be small in comparison to the average time between two implantations at a particular position in the detector, as set by the experimental rates. Off-line analysis of the data allowed the measurement of the average time between implantations into the same position in the silicon detector. The value obtained, $\sim$60 s, is considerably longer than the mean life of the ^{198}Rn isotope which was previously determined to be 92(3) ms [6]. In principle, under the experimental conditions used, good implantation-decay correlations can be found for ^{198}Rn. However, several problems arise in establishing correlated implantation-decay sequences due to the presence of longer-lived isotopes produced at the same time with higher production rates. Difficulties in interpretation arise if two implantations occur at the same position within a time interval which is short in comparison with the half-lives involved. It is not clear under such circumstances with which recoil to associate any subsequent decays seen at that place in the detector. In addition, since the implantation depth of the recoiling ions ($\sim$9–10 μm) is less than the range of α particles in silicon ($\sim$30–40 μm), it is not always possible to detect the decay of every implantation. Only approximately half of the decays are observed with their full energy. In order to minimize these problems, a search is made for a decay at a certain position only within a certain time interval after an implantation. In the final analysis, this time limit was chosen to be 200 ms, although, as discussed below, it is instructive to vary this limit in order to assess contaminant γ-ray transitions arising from residual bad correlations.

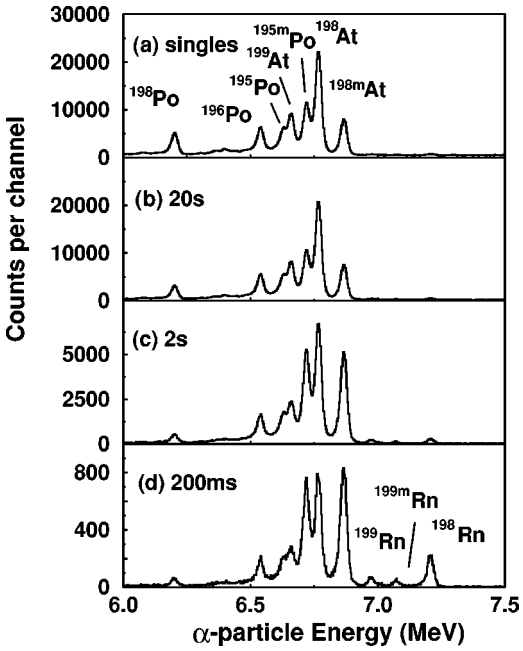

FIG. 1. Energy spectra of α particles associated with (a) any decay event in the strip detector (singles α-particle energy spectrum), (b)–(d) for implantation-decay correlated events with time limits for the correlation of 20 s, 2 s, and 200 ms, respectively; see text for details. Strong α-particle groups are labeled with the decaying isotope.

In addition to implantation-decay sequences, if the daughter isotope is also an α emitter, it is possible to distinguish decays by generation and identify correlations between implantation, first-generation α decay, and second-generation α decay. For the isotopes produced in this reaction, only radon nuclei are expected to show strong first- and second-generation α decays. Other species, such as polonium and astatine, are expected to show only first-generation α decays, since the daughter nuclei undergo β decay. The thickness of the silicon detector is too small to be sensitive to such β particles. In a similar fashion to the time limit discussed above, a time cutoff is applied to the search for a second-generation decay in order to reduce the influence of bad correlations.

IV. RESULTS

The identification of the ^{198}Rn α-particle group was made primarily on the basis of the α-particle energies and half-lives obtained in implantation-decay sequences.

The results of implantation-decay correlations are shown in Fig. 1. The upper portion shows the α-particle energy spectrum for all events in the silicon detector with no correlational analysis performed (referred to below as the singles α-particle energy spectrum). The strongest peaks are labeled by the decaying isotope. This spectrum was calibrated internally using known α-particle energies [11], other than those associated with radon isotopes. The measured α-particle energy from ^{198}Rn decay was 7190(4) keV, in excellent agreement with the previous value of 7196(10) keV [6]. Some

α-particle groups were observed whose presence can only be explained by isotopic contamination in the target. However, there is no evidence for any reactions on erbium isotopes lighter than $A=166$. The group associated with ^{198}Rn is therefore the highest-energy α decay observed and, as such, is clearly separated from other groups and shows no contamination. It is noted in passing that parent-daughter correlations for this group are consistent with the ^{198}Rn identification.

The lower portions of Fig. 1 show the α-particle spectra associated with decays correlated with an implantation. For each of the spectra, a cutoff was imposed, as discussed above, on the time between the implantation and the decay at a particular position in the silicon. Figures 1(b)–1(d) have time limits of 20 s, 2 s, and 200 ms, respectively, which cause changes to the relative intensity of the different α groups in the spectrum depending on the half-life of the decaying isotope. Isotopes, such as ^{198}Rn and ^{199,199m}Rn, with relatively short half-lives, tend to decay before the shortest time cutoff used. Increasing this time cutoff therefore does not significantly increase the number of decays observed. However, the numbers of observed decays associated with isotopes with long half-lives are reduced with application of a time cutoff short in comparison with their half-life. Extending the time cutoff increases the observed number of decays, for example, in Figs. 1(b)–1(d) for ^{198}Po. The correlated spectra in Fig. 1 also show a better peak-to-background in the high α-particle energy region than the singles α-particle energy spectrum. This is due to the removal of the background due to low-energy implantations by the correlation search.

In order to confirm the assignment of the ^{198}Rn group, the distribution of implant-decay times was analyzed in order to measure the associated half-life. Figure 2 shows spectra of the distribution of decay times for radon isotopes observed in the singles α-particle energy spectrum. A maximum likelihood analysis of the decay times gave a measured half-life of 66^{+3}_{-2} ms, which compares well with the previous measurement of 64(2) ms [6]. Half-lives measured for the other radon isotopes produced show a similar consistency with previous results as indicated in Table I.

Once the α-decay groups of interest had been identified, energy spectra were generated of prompt γ rays emitted at the target position by recoiling ions, which subsequently α decay with characteristics associated with particular isotopes. This allows an unambiguous identification of the nuclide associated with particular γ rays.

In order to produce as clean a data set as possible for implantation-decay correlation analysis, implantation events were filtered to reduce the number of events caused by random coincidences between the Ge array and the silicon detector. A polygonal software window was placed around the recoil-ion group in a two-dimensional spectrum of implantation energy versus the time of flight through the separator. This time of flight was measured between the detection of a γ ray and the arrival of the recoiling ion in the silicon detector. This window was shifted along the time axis in order to sample the time-random background and perform a suitable subtraction. In order to gain more insight into the components of the resulting spectra, decay-tagged γ-ray spectra were analyzed for different time cutoffs in the implantation-decay correlation, namely, 20 s, 2 s, and 200 ms.

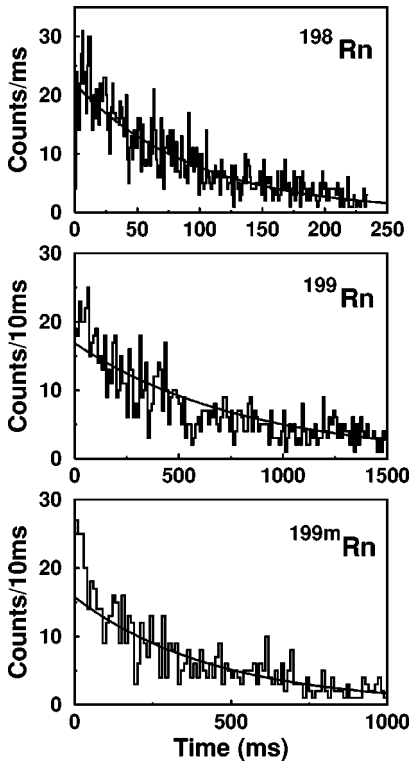

FIG. 2. The distribution of time intervals between the implantation and decay of ^{198}Rn, ^{199m}Rn, and ^{199}Rn ions in the silicon detector. The lines drawn on top of the data are exponential curves corresponding to the half-lives derived from a maximum likelihood analysis of the set of decay times. The exponentials have been superimposed by eye onto the data for illustrative purposes and do not represent a least-squares fit to the number of counts per channel.

Time-random subtracted γ-ray spectra gated by the α group identified as ^{198}Rn are shown in Fig. 3. There are several γ-ray and x-ray transitions apparent in the spectrum which arise in two different ways. The first set of transitions is associated with Coulomb excitation of the ground-state rotational band of the target nucleus ^{166}Er. The 80.6-, 184.4-, and 280.5-keV transitions [11], along with erbium x rays, were initially identified as arising from Coulomb excitation on the basis of the transition energy. These transitions appear in the spectrum from a small number of bad correlations between implantation of ions following Coulomb excitation and some unrelated α decay or a low-energy implantation which has been misinterpreted as an α decay. The mean time between such occurrences is long (of the order of tens of seconds) compared to the decay times for the isotopes of

TABLE I. Measured half-lives, deduced using maximum likelihood estimates from implantation-decay correlations, for radon isotopes. Previous half-life data are taken from Refs. [6] and [11].

Parent isotope	Measured half-life	Previous half-life
^{198}Rn	66^{+3}_{-2} ms	64(2) ms
^{199m}Rn	0.31(2) s	0.325(25) s
^{199}Rn	0.57(3) s	0.620(25) s

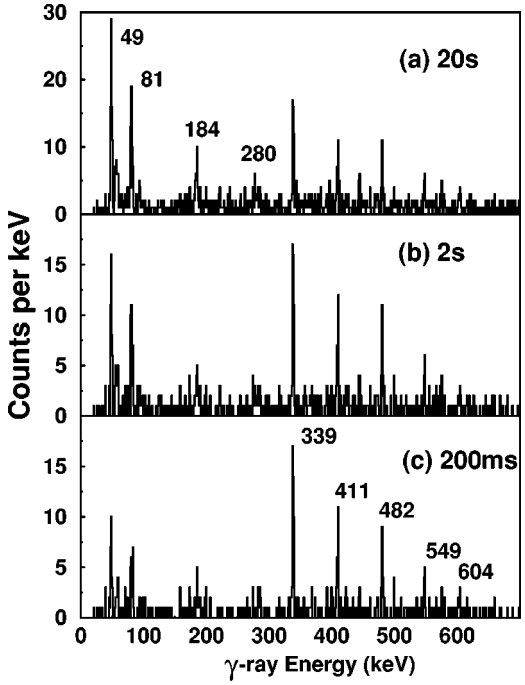

FIG. 3. Energy spectra of prompt γ rays emitted at the target position by ions which subsequently α decay in the strip detector with characteristics associated with ^{198}Rn. In each spectrum a time cutoff has been applied in the implantation-decay correlation. These spectra correspond to time limits of (a) 20 s, (b) 2 s, and (c) 200 ms. Strong peaks are labeled by the transition energy in keV.

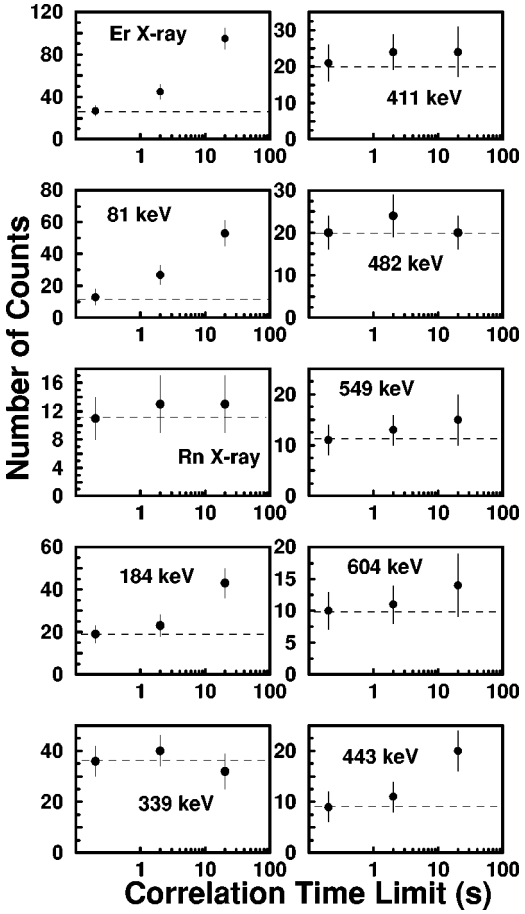

FIG. 4. Graphs showing the number of counts in various peaks in the α-decay tagged γ-ray spectra as a function of the time limit used in the implantation-decay correlation. The data are labeled with the energy of the transition plotted. The x-ray peaks are for erbium $K\alpha$ and radon $K\alpha_1$. The 81-keV yields have the contribution from radon $K\alpha_2$ lines subtracted on the basis of the radon $K\alpha_1$ intensity and the known fluorescence yields [11]. The dashed lines mark the number of counts in the spectrum with a 200 ms time limit in order to guide the eye. Lines arising from the leak through of Coulomb excitation transitions by bad correlation increase above this level with increasing time limit. Transitions associated with ^{198}Rn do not significantly increase as the half-life for this isotope is 64(2) ms, and hence the majority of atoms decay before the 200 ms time limit.

interest. As a result the lines arising as a result of Coulomb excitation appear to grow into the γ-ray spectra with increasing time limit, as can be seen in Figs. 3(a)–3(c) and more quantitatively in Fig. 4. The second group of transitions includes x rays with energies corresponding to radon atoms and a series of distinct γ-ray peaks which are assigned as transitions between excited states in ^{198}Rn. Since the half-life of ^{198}Rn is only 66 ms, the majority of implanted ^{198}Rn ions will decay before the smallest implant-decay time limit used (200 ms). Hence, increasing the time limit will not significantly increase the strength of these lines in the γ-ray spectrum. This characteristic can be used to distinguish ^{198}Rn lines from residual Coulomb excitation breakthrough as illustrated in Fig. 4. A γ-ray transition with an apparent energy of 443 keV shows a linewidth inconsistent with the Coulomb-excitation transitions and has a behavior inconsistent with a mean life of the order of tens of milliseconds. While the origin of this line is unclear, the variation with the implantation-decay time limit rules it out as a candidate transition in ^{198}Rn.

Other γ-ray transitions observed in this reaction which correlate with known α decays are listed in Table II and compared to previous data, if any exist. The comparison of transitions in the current analysis with those from previous work (^{199}At [12], ^{195,195m}Po [13], and ^{196}Po [14]) adds confidence to the analysis performed here. For example, the transitions which correlate with the decay of ^{196}Po compare favorably to those previously measured by more traditional recoil-γ techniques. Transitions have also been observed for the first time which are identified as arising from ^{198}At and ^{198m}At.

The spectrum of ^{198}Rn is characterized by five distinct transitions with energies and relative intensities listed in Table II. The 339.0-keV transition is the strongest and therefore is assumed to be the $2_1^+ \rightarrow 0^+$ transition. There are no other candidates in the measured spectrum between 70 and 400 keV, after considering the effects of efficiency and internal conversion on the apparent intensity. In the absence of γ-γ data, the other transitions are placed on the basis of their relative intensity to give the decay scheme shown in Fig. 5. The spins shown in this diagram are assigned on the basis of systematics illustrated in the next section.

The intensity of the ^{198}Rn group in the singles α-particle energy spectrum, 2384 counts, can be used to estimate the production cross section of ^{198}Rn in this reaction. Several efficiency estimates must be used. The transmission of actinium isotopes through RITU produced in the reaction of

TABLE II. Relative γ-ray intensities obtained in recoil-decay correlated spectra tagged using α groups associated with ^{198}Rn, ^{199}At, ^{198}At, ^{198m}At, ^{195}Po, ^{195m}Po, and ^{196}Po. The measured transition energies are compared to previous results where possible taken from the Refs. [12–14]. Intensities are corrected for the effects of relative efficiency only. Errors quoted on observed energies are purely statistical. Contributions of systematic error to the measured energies are discussed in the text.

	Transition energy (keV)	Intensity	Previous energy (keV)
^{198}Rn			
	339.0(2)	100(15)	
	410.5(3)	68(13)	
	481.5(3)	58(13)	
	548.8(5)	34(10)	
	604.0(8)	27(9)	
^{199}At			
	433.2(1)	53(8)	432.9
	600.5(3)	100(14)	
	610.1(7)	22(8)	608.2
	655.8(5)	19(4)	
	671.0(2)	44(9)	
	700.6(7)	11(3)	
^{198}At			
	130.0(1)	64(9)	
	136.7(2)	21(5)	
	151.7(2)	20(7)	
	155.5(9)	38(10)	
	168.3(1)	33(6)	
	173.7(2)	14(4)	
	247.5(1)	54(8)	
	279.1(2)	75(12)	
	284.4(1)	100(14)	
	304.9(5)	34(9)	
	422.2(2)	17(6)	
	486.5(4)	31(9)	
	566.2(4)	42(11)	
^{198m}At			
	136.2(2)	7(2)	
	247.4(1)	30(5)	
	279.1(3)	23(6)	
	284.1(1)	81(10)	
	413.3(2)	18(5)	
	422.2(2)	53(9)	
	551.9(1)	31(6)	
	567.1(1)	100(14)	
^{195}Po			
	243.8(2)	60(15)	
	319.1(3)	48(14)	319(1)
	401.8(6)	63(21)	402(1)
	405.9(3)	64(19)	
	428.4(3)	100(24)	427(1)
	470.8(5)	95(20)	470(1)
	488.3(3)	30(12)	
	495.1(4)	37(14)	494.8(1)
	498.6(3)	61(19)	
	600.5(4)	62(20)	
^{195m}Po			
	319.5(2)	100(6)	318.7(5)
	388.9(2)	52(4)	388.4(5)
	403.8(4)	9(2)	
	427.3(3)	11(2)	
	495.0(3)	31(4)	494.8(5)
^{196}Po			
	237.6(2)	20(3)	237.3(1)
	254.1(2)	17(1)	253.4(1)
	277.8(5)	11(3)	
	283.8(4)	15(4)	
	388.9(3)	20(5)	387.6(1)
	396.8(3)	17(4)	395.8(1)
	404.8(6)	14(4)	
	414.1(3)	31(5)	414.2(8)
	427.5(2)	86(10)	427.9(1)
	432.3(3)	15(4)	
	462.7(2)	100(11)	463.1(1)
	498.1(2)	67(9)	499.1(1)
	517.6(4)	9(3)	
	528.1(3)	17(5)	528.6(1)
	582.6(3)	35(6)	583.9(2)
	615.4(6)	21(6)	616.9(2)

^{40}Ar beams with ^{175}Lu targets at 185 MeV has been measured [15] to be between 25% and 35%. The reaction used here is similar and RITU transmission has been assumed to be 30%. Comparisons of the number of recoil-decay correlated ^{198}Rn events and the number of second generation recoil-decay-decay events indicate that the efficiency of measuring an α particle which deposits its full energy into the

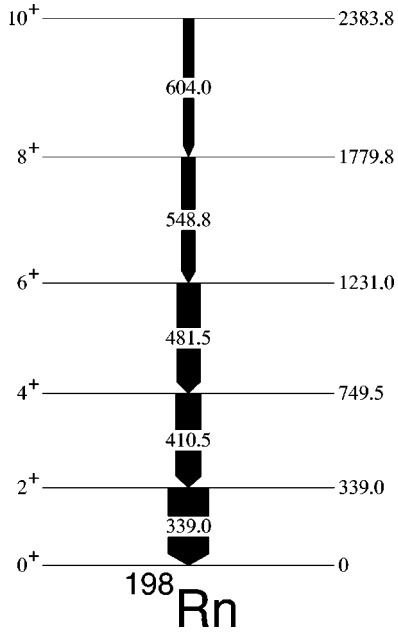

FIG. 5. The decay scheme of ^{198}Rn derived from the current work. See text for details of assignments.

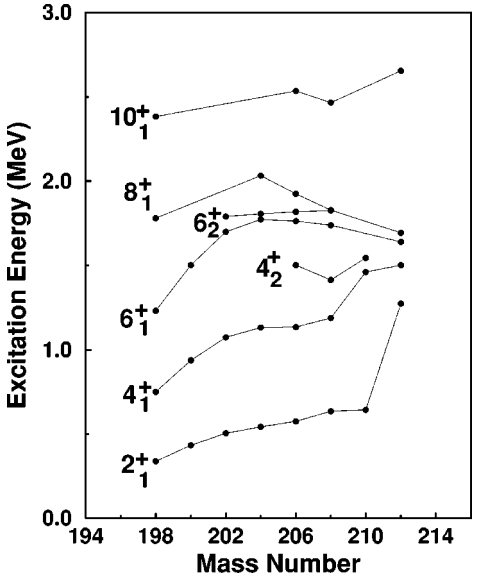

FIG. 6. Excitation energies of low-lying states in neutron-deficient radon isotopes with $N \leq 126$. The data are taken from Refs. [16–22].

silicon detector is ~67%. This figure is in line with that expected on the basis of simple geometric estimates involving implantation depth and α-particle range in silicon. On this basis the production cross section for ^{198}Rn is 180 nb. This must be viewed only as an estimate due to the uncertainty in some of the experimental parameters. A similar analysis using the intensity of the 339.0-keV transition, 46 counts, and an estimated γ-ray efficiency at that energy of 4% (made on the basis of the measured absolute efficiency at 1332 keV and the measured relative efficiency curve) gives a lower value for the cross section. This indicates that excited states in some of the ^{198}Rn nuclei produced decay via isomers with half-lives longer than a few tens of nanoseconds.

V. INTERPRETATION AND CONCLUSIONS

The low-lying systematics of excited states in even-mass radon isotopes below the $N=126$ shell closure are illustrated in Fig. 6. The data are those obtained in the current work for ^{198}Rn compared with those for heavier isotopes from Refs. [16–22]. The low-lying levels of the singly closed shell nucleus ^{212}Rn are predominately based on $\pi h^4_{9/2}$ structures. In more neutron-deficient isotopes, increasing neutron degrees of freedom make more configurations available at low excitation energy, thus increasing admixtures of other configurations in the $\pi h^4_{9/2}$ states. The gradual fall in excitation energy of the 2^+_1 and 4^+_1 states, in increasingly neutron-deficient isotopes out to $A=202$, can be attributed to the increase in collectivity of the low-lying levels. This mechanism is also responsible for the increase in the transition probability of the 8^+_1 isomers when moving away from the $N=126$ closure. Beyond $A=202$, both the 4^+_1 and 6^+_1 states show a rather more dramatic fall in excitation energy with decreasing neutron number. The slight initial rise in the energy of the 6^+_1 and 8^+_1 states in moving from $A=214$ to $A=204$ compared to the rather steep fall in isotopes with $A<204$, is suggestive of different structures for these states in isotopes near to the $N=126$ closure, compared to those with larger neutron deficiency. It is interesting to note that there is little information on 10^+_1 states in these nuclei. A candidate for the 10^+_1 state is apparent from this work in ^{198}Rn, but ^{200}Rn is only known up to spin 4^+, with a tentative spin-6 state [16].

It is clear that naive conclusions drawn from the results of theoretical calculations [1–4]—that radon isotopes with mass numbers lighter than 202 have permanent ground-state shapes corresponding to a deformation parameter, $|\epsilon_2|=0.2$—are not substantiated by the current data. Axial deformation of this extent should result in a first excited state at an excitation energy of just over 100 keV and a reasonably well-developed rotational ground-state band. In contrast, ^{198}Rn has a first excited state at 339 keV and the ratio $E(4^+)/E(2^+)$ has a value of 2.2. This is more typical of an anharmonic vibrator than of a clearly defined rotational band, which is expected to exhibit a ratio of 3.33. Similar inconsistency has been seen in the low-lying levels of ^{200}Rn [16]. The problem of theoretically describing the ground-state shapes in this region therefore needs readdressing.

The excited states may, however, suggest the influence of deformation in the lighter isotopes. The steep fall in the excitation energy of higher-lying states in radon isotopes with increasing neutron deficiency for $A<204$ is suggestive of the spherical $\pi h^4_{9/2}$ structures close to $A=212$ being crossed by states whose structure is quite different and which become energetically favored with increasing numbers of neutron holes. Below $Z=82$, similar behavior is known to be associated with deformed intruder configurations which fall in excitation energy with decreasing neutron number away from $N=126$. In platinum isotopes, which have the same number of valence protons with respect to $Z=82$ as radon isotopes, sufficiently neutron-deficient nuclides are known for the characteristic parabolic variation of the energy of the intruder states to be mapped out [23]. In the midshell region, at the minimum of the parabola, the ground-state wave function has significant admixtures of the deformed structure. Such an interpretation for $Z=78$ and $Z=80$, where similar features are observed, has supporting evidence from measurements of transition quadrupole moments and rotational band structures.

Above $Z=82$ the evidence for the presence of deformed intruder configurations is less clear, although recent energy systematics in polonium isotopes do suggest that similar effects occur. A measurement of the low-lying structure of ^{192}Po [24] indicates that the minimum of the parabolic variation is being approached and that the ground-state wave function should therefore contain admixtures of the intruding configuration. Such conclusions are strengthened by α-decay studies of radon isotopes which observe population of 0^+_2 states in the polonium daughters [6]. Interpretation of such states in terms of deformed intruder states indicates that strong mixing into the ground state does occur in ^{192,194}Po. It must be noted, however, that the low-lying structure of the neutron-deficient polonium isotopes has also been interpreted with some success using particle-vibration coupling without the need for deformed particle-hole excitations [25].

The radon energy-level systematics are therefore suggestive of falling intruder configurations with increasing number of neutron holes. Comparison with the polonium systematics indicates that a flattening of the fall in the energy of the 4^+ and 6^+ states, which could be associated with significant mixing of intruder and ground-state configurations, may occur for more neutron-deficient isotopes. Such conclusions remain rather speculative as supporting evidence is lacking. Studies of such neutron-deficient isotopes as ^{198}Rn are at the very limit of current in-beam γ-ray spectroscopy since the production reaction has a cross section of the order of 100 nb, the smallest ever used in such work, and as such, supporting evidence is difficult to obtain. The extension of the current energy systematics to lighter radon isotopes is also difficult. While the α-decay characteristics of ^{196}Rn have recently been established [26], the production cross section is only at the level of a few nanobarns. Such measurements are only possible by employing a state-of-the-art array of germanium detectors, with a photopeak efficiency approaching 10%, at the target position of a high-transmission, and therefore necessarily gas-filled, separator.

In conclusion, the low-lying levels of ^{198}Rn have been established for the first time using in-beam γ-ray spectroscopy. The reaction used has a production cross section of only 180 nb. The isolation and identification of radiation from such weakly produced evaporation residues was only possible by correlation with radioactive decay, in order to remove the vastly more intense backgrounds from fission and Coulomb excitation. The structure of ^{198}Rn is inconsistent with theoretical predictions of a sizable permanent ground-state deformation, while energy systematics are suggestive of the presence of intruder configurations which fall in energy with increasing neutron deficiency.

ACKNOWLEDGMENTS

This work was supported by the U.K. Engineering and Physical Sciences Research Council (EPSRC), the Academy of Finland and by the Access to Large Scale Facility program under the Training and Mobility of Researchers program of the European Union. R.B.E.T. and S.D.R. acknowledge support of the EPSRC.

[1] E. Marshalek, L. Person, and R.K. Sheline, Rev. Mod. Phys. **35**, 108 (1963).

[2] P. Möller and J.R. Nix, At. Data Nucl. Data Tables **26**, 165 (1981).

[3] R. Bengtsson, P. Möller, J.R. Nix, and J. Zhang, Phys. Scr. **29**, 402 (1984).

[4] P. Möller, J.R. Nix, and W.J. Swiatecki, At. Data Nucl. Data Tables **59**, 185 (1995).

[5] F. Calaprice, G.T. Ewan, R.-D. von Dincklage, B. Jonson, O.C. Jonsson, and H.L. Ravn, Phys. Rev. C **30**, 1671 (1984).

[6] N. Bijnens, P. Decrock, S. Franchoo, M. Gaelens, M. Huyse, H.-Y. Hwang, I. Reusen, J. Szerypo, J. von Schwarzenberg, J. Wauters, J.G. Correia, A. Jokinen, P. Van Duppen, and the ISOLDE Collaboration, Phys. Rev. Lett. **75**, 4571 (1995).

[7] P.J. Nolan, F.A. Beck, and D.B. Fossan, Annu. Rev. Nucl. Part. Sci. **45**, 561 (1994).

[8] P.J. Nolan, D. Gifford, and P.J. Twin, Nucl. Instrum. Methods Phys. Res. A **236**, 95 (1995).

[9] M. Leino, J. Äystö, T. Enqvist, P. Heikkinen, A. Jokinen, M. Nurmia, A. Ostrowski, W.H. Trzaska, J. Uusitalo, K. Eskola, P. Armbruster, and V. Ninov, Nucl. Instrum. Methods Phys. Res. B **99**, 653 (1995).

[10] A. Ghiorso, S. Yashita, M.E. Leino, L. Frank, J. Kalnins, P. Armbruster, J.-P. Dufour, and P.K. Lemmertz, Nucl. Instrum. Methods Phys. Res. A **269**, 192 (1988).

[11] E. Browne and R.B. Firestone, in *Table of Radioactive Isotopes*, edited by V.S. Shirley (Wiley, New York, 1986).

[12] K.-M. Spohr, Ph.D. thesis, Institut für Kernphysik, Jülich-3171, Germany, Report No. ISBN-0944-2952, 1996.

[13] N. Fotiades, J.A. Cizewski, D.P. McNabb, K.Y. Ding, C.N. Davids, R.V.F. Janssens, D. Seweryniak, M.P. Carpenter, H. Amro, P. Decrock, P. Reiter, D. Nisius, L.T. Brown, S. Fischer, T. Lauritsen, J. Wauters, C.R. Bingham, M. Huyse, A. Andreyev, and L.F. Conticchio, Phys. Rev. C **56**, 723 (1997).

[14] L.A. Bernstein, J.A. Cizewski, H.-Q. Jin, R.G. Henry, L.P. Farris, A. Charos, M.P. Carpenter, R.V.F. Janssens, T.L. Khoo, T. Lauritsen, I.G. Bearden, D. Ye, J.A. Becker, E.A. Henry, M.J. Brinkman, J.R. Hughes, A. Kuhnert, T.F. Wang, M.A. Stoyer, R.M. Diamond, F.S. Stephens, M.A. Deleplanque, A.O. Macchiavelli, I.Y. Lee, B. Cederwall, J.R.B. Oliveira, J. Burde, P. Fallon, C. Duyar, J.E. Draper, E. Ribel, and D.T. Vo, Phys. Rev. C **52**, 621 (1995).

[15] Juha Uusitalo, Ph.D. thesis, University of Jyväskylä, Report No. ISBN 951-34-0798-5, 1996.

[16] R.B.E. Taylor, S.J. Freeman, J.L. Durell, M.J. Leddy, A.G. Smith, D.J. Blumenthal, M.P. Carpenter, C.N. Davids, C.J. Lister, R.V.F. Janssens, and D. Seweryniak, Phys. Rev. C **54**, 2926 (1996).

[17] S.J. Freeman, A.G. Smith, S.J. Warburton, B.B. Back, I.G. Bearden, D.J. Blumenthal, M.P. Carpenter, B. Crowell, C.N. Davids, D. Henderson, R.V.F. Janssens, T.L. Khoo, T. Lauritsen, C.J. Lister, D. Nisius, H.T. Penttila, J.A. Becker, P. Chowdhury, and E.F. Moore, Phys. Rev. C **50**, 1754 (1994).

[18] D. Horn, C. Baktash, and C.J. Lister, Phys. Rev. C **24**, 2136 (1981).

[19] B.G. Ritchie, F.T. Avignone III, H.K. Carter, R.L. Mlekodaj, and E.H. Spejewski, Phys. Rev. C **23**, 1717 (1981).

[20] W.J. Triggs, A.R. Poletti, G.D. Dracoulis, C. Fahlander, and A.P. Byrne, Nucl. Phys. **A395**, 274 (1983).

[21] A.R. Poletti, G.D. Dracoulis, C. Fahlander, and I. Morrison, Nucl. Phys. **A380**, 335 (1982).

[22] G.D. Dracoulis, P.M. Davidson, A.P. Byrne, B. Fabricius, T. Kibedi, A.M. Baxter, A.E. Stuchberry, A.R. Poletti, and K.J. Schiffer, Phys. Lett. B **246**, 31 (1990).

[23] J.L. Wood, K. Heyde, W. Nazarewicz, M. Huyse, and P. Van Duppen, Phys. Rep. **215**, 101 (1992).

[24] K. Helariutta, T. Enqvist, P. Jones, R. Julin, S. Juutinen, P. Jämsen, H. Kankaanpää, P. Kuusiniemi, M. Leino, M.

Muikku, M. Piiparinen, A. Savelius, W.H. Trzaska, S. Törmänen, J. Uusitalo, R.G. Allat, P.A. Butler, P.T. Greenlees, and R.D. Page, Phys. Rev. C **54**, R2799 (1996).

[25] W. Younes and J.A. Cizewski, Phys. Rev. C **55**, 1218 (1997).

[26] Y.H. Pu, K. Morita, M.G. Hies, K.O. Lee, A. Yoshida, T. Nomura, Y. Tagaya, T. Motobayashi, M. Kurokawa, H. Minemura, T. Uchibori, T. Argia, K. Sueki, and S.A. Shin, Z. Phys. A **357**, 1 (1997).